Theor Chem Acc (2002) 108:255–272
DOI 10.1007/s00214-002-0364-8

Theoretical Chemistry Accounts

Feature article

Breathing-orbital valence bond method – a modern valence bond method that includes dynamic correlation

Philippe C. Hiberty[1], **Sason Shaik**[2]

[1]Laboratoire de Chimie-Physique, Groupe de Chimie Théorique, Université de Paris-Sud, 91405 Orsay Cedex, France
[2]Department of Organic Chemistry and Lise Meitner-Minerva Center for Computational Chemistry, Hebrew University, 91904 Jerusalem, Israel

Received: 4 March 2002 / Accepted: 20 May 2002 / Published online: 23 October 2002

Abstract. This account describes the breathing-orbital valence bond (BOVB) method, a modern valence bond method that incorporates differential dynamic correlation associated with the bond making and breaking of a chemical event. The method aims to combine the properties of interpretability and compactness of the classical valence bond method with good accuracy of the energetics. The domain of applicability of the BOVB method is mainly for problems that require interpretation of an electronic wave function in terms of Lewis structures. The method generates all the covalent and ionic Lewis structures that are relevant to the electronic state, and represents each of them by a single valence bond configuration state function. A balanced description of the different Lewis structures is then ensured by allowing each configuration to have its specific set of orbitals during the optimization process. In this framework, the dynamic correlation associated with the breaking or forming of a bond is viewed as the instantaneous adaptation of the orbitals to the electron fluctuation inherent to the bond; hence, the ''breathing orbital'' characterization. Applications of the BOVB method to a variety of problems are described, for example, two-electron bonds, odd-electron bonds, bonds to transition metals, resonance energies, and diabatic surfaces. In all these applications, the method is shown to provide bonding energies that compare well to accurately calculated or experimental values, despite the extreme compactness of the wave functions.

Key words: Valence bond – Dynamic electron correlation – Breathing orbitals – Diabatic states – Resonance energy

1 Introduction

Despite the dominance of the molecular orbital (MO) method for computational purposes, much of chemical wisdom is still couched in terms of valence bond (VB) concepts, such as local bonds and lone pairs, which are key elements of the Lewis concept of the chemical bond [1, 2]. Thus, a chemical bond involves spin-pairing of electrons, which occupy valence atomic orbitals (AOs) or hybrids of adjacent atoms that are bonded in the Lewis structure. In this manner, each term of a VB wave function corresponds to a specific chemical formula or Lewis structure, and has thereby a clear qualitative significance. As such, VB theory and its simplest variant, resonance theory [3], have generated fundamental concepts such as hybridization, covalency, ionicity, resonance hybrid species, resonance stabilization, and so on. These concepts served chemists extremely well and enabled them to rationalize and predict reaction mechanisms or molecular properties by simply writing down VB structures on a back of an envelope.

Alongside this historical significance, contemporary VB theory offers a quantitative means for studying a variety of problems [4] at the level of a unique chemical insight that is not available by standard ab initio MO-based computations. This unique insight originates from the ability of VB theory to construct diabatic states, which represent electronic structures that are as invariant as possible throughout a reaction coordinate. The diabatic states so generated apply to numerous problems, such as

1. Chemical dynamics, in cases where the Born–Oppenheimer approximation breaks down.
2. Chemical reactivity, with the Shaik–Pross diagrams, in which a reaction barrier originates in the avoided crossing of two diabatic state curves, one representing the generalized bonding scheme of the reactants and the other that of the products [5, 6].

This paper is dedicated to H. Schwarz on occasion of his 60th birthday.

Correspondence to: P. C. Hiberty
e-mail: philippe.hiberty@lcp.u-psud.fr

3. Photochemistry, with harpooning and charge-transfer mechanisms [7], and photochemical funnels [8].
4. Fundamental principles of organic chemistry, for example, the role of electronic delocalization as a stabilizing factor [9, 10, 11, 12].
5. Solvation, with theoretical models treating the solvation effects separately on covalent and ionic components of a bond [13].

For such applications, it is not only important to be able to interpret the wave function in terms of chemical structural formulas (Lewis structures), but also to estimate the energy of each of these individual Lewis structures and their variations along a reaction coordinate prior to their interaction to form the adiabatic states. This requires computational VB methods that combine quantitative rigor and conceptual clarity. We can define therefore the following wish list for a VB method:

1. Unambiguous interpretability of the wave function in terms of Lewis structures.
2. Compactness of the wave function.
3. Ability to calculate diabatic as well as adiabatic states.
4. Accounting for dynamic correlation to give reasonable accuracy (say a few kilocalories per mole) of the calculated energetics.
5. Consistency of the accuracy at all points of the surfaces calculated.

The latter two points on the wish list require the method to be able to describe the elementary events of a reaction, i.e., bond-breaking or bond-forming, in a faithful manner. Thus, a crucial test for the method will be its ability to reproduce dissociation curves, for two-electron as well as odd-electron bonds. This account focuses on a VB methodology, the so-called breathing orbital VB (BOVB) method, which was recently developed [14, 15, 16, 17] with these essential features in mind, and which has been successfully applied to a variety of chemical problems [18–24].

2 VB theory and electron correlation

The term "electron correlation energy" is very simply defined in the MO framework. It is the difference between the exact nonrelativistic energy and the energy provided by the simplest MO wave function, the monodeterminantal Hartree–Fock wave function. Within this definition, it is customary to distinguish between nondynamic and dynamic electron correlation.

2.1 Coulomb (static) electron correlation

Coulomb electron correlation is the part of the total correlation energy that is included in a complete-active-space self-consistent field (CASSCF) calculation, which correlates the valence electrons in valence orbitals. In VB terms, the Coulomb correlation ensures a correct balance between the ionic and covalent components of the wave function for a given electronic system [25]. The dynamic correlation is just what is still missing to get the exact nonrelativistic wave function.

The essential part of Coulomb correlation energy for polyatomic molecules is the " left–right electron correlation", which is concerned with the ionic–covalent balance within a given two-electron bond. Let us therefore discuss this type of correlation in the case of a homonuclear single bond that links together two AOs, χ_a and χ_b, of some identical atoms A and B.

A VB wave function that takes care of left–right correlation is Ψ_{VB} in Eq. (1), in which the coefficients λ and μ are optimized to minimize the total molecular energy. Here the first term in parentheses is purely covalent, and is often called the Heitler–London (HL) wave function (Ψ_{HL}) by analogy with the first historical VB calculation of H_2 by Heitler and London [26] in 1927. The second term is the ionic component of the bond, which is present in all bonds.

$$\Psi_{VB} = \lambda(|\chi_a\bar{\chi}_b| + |\chi_b\bar{\chi}_a|) + \mu(|\chi_a\bar{\chi}_a| + |\chi_b\bar{\chi}_b|) \quad (1)$$

This description of the A–B bond corresponds to the classical VB method if χ_a and χ_b are just the orbitals of the free atoms and corresponds to the VBSCF method [27] if both coefficients λ and μ as well as the orbitals are simultaneously optimized in a flexible basis set. This method can be readily extended to polyatomic molecules, simply by generating a complete and linearly independent set of covalent and ionic structures for the molecule at hand. As this set of VB structures generates the same configurational space as the set of valence CASSCF configurations in the MO framework, such a VB calculation takes into account all the Coulomb correlation of the molecule. Thus, a complete VBSCF calculation that deals with pure AOs is conceptually equivalent to a valence CASSCF calculation, although this equivalence is only approximate in flexible basis sets, the VBSCF energy being slightly higher. Now a severe inconvenience of describing each bond of a polyatomic molecule by one covalent and two ionic components is that the number of VB structures grows exponentially with the size of the molecule. In light of this difficulty, Coulson and Fischer [28] proposed an elegant way to incorporate left–right correlation into a single and formally covalent VB structure of the HL type. They used slightly delocalized orbitals as exemplified for the A–B bond in Eq. (2), dropping the normalization constants.

$$\Psi_{CF} = |\varphi_l\bar{\varphi}_r| + |\varphi_r\bar{\varphi}_l|, \quad \varphi_l = \chi_a + \varepsilon\chi_b,\ \varphi_r = \chi_b + \varepsilon\chi_a \quad (2)$$

Here each orbital, φ_l or φ_r, is mainly localized on a single center but involves a small tail on the other center, so the expansion of the Coulson–Fischer (CF) wave function Ψ_{CF} (Eq. 3) in AO determinants is in fact equivalent to Ψ_{VB} in Eq. (1), provided the coefficient ε is properly optimized.

$$\Psi_{CF} = (1+\varepsilon^2)(|\chi_a\bar{\chi}_b| + |\chi_b\bar{\chi}_a|) + 2\varepsilon(|\chi_a\bar{\chi}_a| + |\chi_b\bar{\chi}_b|) \quad (3)$$

In the generalized VB (GVB) method [29, 30], each bond in a polyatomic molecule is described in the CF way, i.e., the bond is considered as a pair of nonorthogonal and spin-coupled orbitals, as in the HL wave function. In the early version of this method [30], all

possible spin couplings were allowed for a unique set of spatial orbitals, and no orthogonality restrictions were imposed on the orbitals. For the sake of computational efficiency, the different GVB pairs were later constrained to be mutually orthogonal, without much loss of numerical accuracy. The resulting GVB wave function that formally displays purely covalent bonds implicitly contains ionic structures, necessary for a reasonable description of the bonds. The most popular version of GVB theory is the so-called "perfect pairing" approximation, which considers a single spin-coupling scheme which reflects the way AOs are bonded together in the Lewis structure. A method that relies on the same philosophy is the spin-coupled (SC) theory [31]; however, like the early GVB versions, this method removes any orthogonality restrictions and considers all possible spin-coupling schemes between the singly occupied orbitals. The lone pairs can be treated either as doubly occupied localized orbitals, or as pairs of strongly overlapping singly occupied orbitals.

The GVB and SC methods take care of the left–right correlation for each bond of a polyatomic molecule; however, these methods do not include the totality of the Coulomb correlation since the various local ionic situations are not interconnected with these methods. For example, the two ionic situations **1** and **2** (Scheme 1) are expected to have different weights, the weight of **2** being more important than **1**, but this feature is not taken into account in the wave functions based on CF orbitals. To include all nondynamic electron correlation, one should abandon the CF idea and go back to VB structures constructed with strictly localized AOs, without any delocalization tails, and generate all possible VB structures, allowing their coefficients and orbitals to be optimized simultaneously.

Technically, the simultaneous optimization of orbitals and coefficients for a multistructure VB wave function can be done with the VBSCF method due to van Lenthe and Balint-Kurti and Benneyworth [27] and Verbeek and coworkers [32, 33]. The VBSCF method has the same format as the classical VB method with the important difference that while the classical VB method uses orbitals that are optimized for the separate atoms, the VBSCF method uses a variational optimization of the AOs in the molecular wave function. In this manner the AOs adapt themselves to the molecular environment with a resulting significant improvement in the total energy and other computed properties.

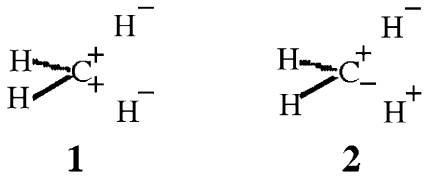

1 **2**

Scheme 1

2.2 Dynamic electron correlation

The importance of left–right correlation for the description of the bond is best appreciated in the case of the F_2 molecule. Here the experimental bonding energy is 38 kcal/mol, while the Hartree–Fock bond energy is negative, –36 kcal/mol [34], i.e., the energy of the molecule is found to be higher than that of the separated fluorine atoms. The situation improves considerably at the GVB, VBSCF, or CASSCF level (Tables 1, 2), which are roughly equivalent for this molecule. However, despite the improvement, the calculated bonding energy is still disappointingly small, reaching only half the full configuration interaction (CI) estimate with the same basis set. Thus, while GVB and VBSCF (and CASSCF) calculations take care of the Coulomb correlation, they do not treat the dynamic correlation which is accounted for in the extensive CI calculation. The qualitative defect of the GVB, VBSCF, or CASSCF wave function of F_2 appears instantly once the wave function is expanded in terms of covalent and ionic VB structures with strictly localized AOs, in a manner similar to Eq. (3), and as pictorially represented in Scheme 2.

In the GVB and VBSCF wave functions the orbitals and coefficients of the covalent and ionic structures are optimized. However, the AOs are nearly identical for the covalent and ionic structures, i.e., the orbitals are adapted to the mean field of the three structures. In fact, all the orbitals are optimized for an average neutral situation, which is about correct for the covalent structure but disfavors the ionic ones. Now common sense suggests that the molecular energy would be further lowered if the AOs were allowed to assume different sizes and shapes, depending on whether they belong to the neutral atoms in the covalent structure or to the ionic atoms in the ionic structures. One can therefore anticipate that the mean-field constraint of the GVB and VBSCF methods will underestimate the weight of the ionic structures, leading to an inaccurate description of the bond. Relaxing this constraint during the orbital optimization should allow each VB structure to have its own specific set of orbitals, different from one structure to the other, and would improve the description of the bond without increasing the number of VB structures. In such a wave function, the orbitals can be viewed as instantaneously following the charge fluctuation by rearranging in size and shape. Such orbitals were dubbed "breathing orbitals" and the method itself was named the

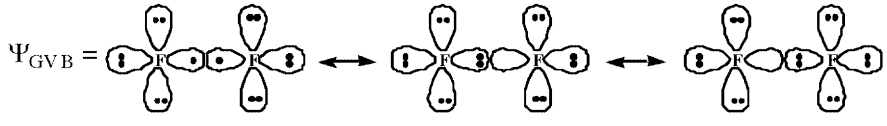

$F\bullet\!-\!\bullet F$ $F^-\ F^+$ $F^+\ F^-$

Scheme 2

"breathing-orbital VB" (BOVB) method. Our working hypothesis is that the improvement brought by this BO effect closely corresponds to the contribution of dynamic correlation to the formation of the bond. Thus, in the BOVB picture the dynamic correlation derives from the wave property of the electron that enables the electronic density to respond instantaneously to the varying local charges in the VB structures.

3 The BOVB method

The idea of using different orbitals for different VB structures is not new, and has been successfully applied to molecules qualitatively represented as a pair of resonating degenerate Lewis structures, for example, formyloxyl radical, carboxylate anions, etc. [35, 36, 37]. In this context, the nonorthogonal CI of Jackels and Davidson for the formyloxyl radical [35], the RGVB method of Voter and Goddard [36], and the generalized multistructural wave function of Nascimento [37] should be mentioned. Murphy and Messmer [38] developed a novel GVB method in which the local orbitals are allowed to be different for different spin-couplings, an improvement which makes the wave function attain nearly all of the correlation energy of a corresponding CASSCF calculation. What we advocate here is just the systematic application of the principle of different orbitals for different VB structures to the description of the chemical bonds, the latter being described with explicit inclusion of their covalent and ionic components.

3.1 General principles

The general philosophy is that the representation of an electronic state in terms of Lewis structures is not just a model but rather an intimate picture of the true nature of the chemical interactions. The picture needs only a rigorous quantum mechanical formulation to become a quantitative computational method. The procedure that derives from this philosophy and underlies the BOVB method is straightforward. It consists of generating all the Lewis structures that are necessary to qualitatively describe a reacting system in VB terms and providing the corresponding VB structures with the best possible orbitals to minimize the energy of the final multistructure state. This kind of "absolute" optimization of the orbitals is attained by getting rid of the previously discussed mean-field constraint (e.g., of GVB, VBSCF, etc.), and allowing different orbitals for different VB structures. The method is thus grounded on the basic postulate that if all relevant Lewis structures of an electronic state are generated and if these are described in a balanced way by a wave function, then this wave function should accurately reproduce the energetics of this electronic state throughout a reaction coordinate.

The requirement that all Lewis structures be generated requires in turn that both covalent and ionic components of the chemical bonds have to be considered. As the number of VB structures grows exponentially with the number of electrons, it is apparent that the BOVB method will not be applied to large systems of electrons, but rather to that small part of a molecular system that effectively "participates" in a reaction, the so-called "active subsystem". The rest of the electrons are considered as spectators that are treated at the MO level, but their MOs are allowed to undergo optimization during the BOVB procedure.

3.2 Choice of an active subsystem

Consider a typical S_N2 reaction as an example (Eq. 4). The reaction consists of the breaking of a C–F bond followed by the formation of a new C–Cl bond.

$$Cl^- + CH_3{-}F \rightarrow [Cl{-}CH_3{-}F]^- \rightarrow Cl - CH_3{+}F^- \quad (4)$$

The four electrons and three orbitals involved in the C–F bond and in the attacking lone pair of Cl^- will constitute the core of the reaction, and will form the "active" system. Three lone pairs of fluorine, three other lone pairs of chlorine, and three C–H bonds of carbon will keep their status unchanged during the reaction and will form the "inactive" system. Generally, the active system will be composed of those orbitals and electrons that undergo bond-breaking or bond-forming in a reaction. While the inactive system will be treated as localized doubly occupied MOs at the MO level, the active system will, in contrast, be subject to a detailed VB treatment involving the complete set of chemically relevant Lewis structures.

In this example, this would mean consideration of the set of the six VB structures (**3–8**) that one can construct for a system of four electrons in three orbitals (Scheme 3).

The active electrons are thus explicitly correlated (by Coulomb correlation), while the inactive electrons are not. One expects that the lack of Coulomb correlation in the inactive subsystem will result in a constant error throughout the potential surface and therefore just uniformly shift the calculated energies relative to the fully correlated surface. Note that in this model all the occupied orbitals, active and inactive, are affected by the progress of the reaction, and thereby rearrange and adapt themselves to the local charges of the VB structures and to their mixing at all points of the reaction coordinate.

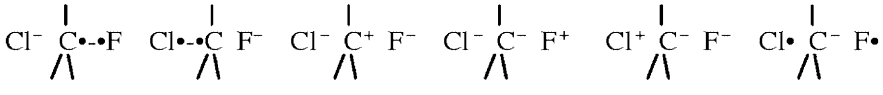

3 **4** **5** **6** **7** **8**

Scheme 3

The previous definitions of active/inactive subsystems are of course not restricted to the study of reactions but can be generalized to all species whose qualitative description can be made in terms of resonating Lewis structures, such as conjugated molecules, mixed valence compounds, etc.

3.3 VB formulation of the Lewis structures

After the choice of the relevant Lewis structures has been made, the following step involves their quantum mechanical formulation. Each Lewis structure corresponds to a set of AOs which are singly or doubly occupied, as illustrated in **9–11** for the F_2 molecule (Scheme 4).

Each such Lewis structure is represented by a single VB spin eigenfunction (Ψ_9–Ψ_{11}), called a "VB structure". These VB structures are linear combinations of Slater determinants involving the same occupied AOs as the corresponding Lewis structures, as in Eqs. (5), (6), and (7):

$$\Psi_9 = |\ldots \varphi_i \ldots L_n \bar{R}_n| + |\ldots \varphi_i \ldots R_n \bar{L}_n| \ , \tag{5}$$

$$\Psi_{10} = |\ldots \varphi_i' \ldots L_a \bar{L}_a| \ , \tag{6}$$

$$\Psi_{11} = |\ldots \varphi_i'' \ldots R_a \bar{R}_a| \ . \tag{7}$$

Here φ, φ', and φ'' represent the set of inactive orbitals for each VB structure, L and R are the active orbitals of the left and right fragments, respectively, and the subscripts n and a stand for neutral and anionic fragments, respectively (recall that the cationic fragments have only inactive orbitals and no active ones). Note that the inactive orbitals φ_i, φ_i' and φ_i'' of Ψ_9–Ψ_{11} are all different from each other, as are the active orbitals L_n, L_a, or R_n, R_a. These differences are pictorially represented in **9–11** by drawing orbitals with different sizes depending on the identity of the species as neutral, cationic, or anionic, but the orbitals may also differ in shape (e.g., different angular properties owing to rehybridization).

An important feature of the BOVB method is that the active orbitals are chosen to be strictly localized on a single atom or fragment, without any delocalization tails. If this were not the case, a so-called "covalent" structure, defined with slightly delocalized orbitals like, for example, CF orbitals, would implicitly contain some ionic contributions, which would make the interpretation of the wave function questionable [39]. The use of pure AOs is therefore a way to ensure unambiguous correspondence between the concept of the Lewis structural scheme and its mathematical formulation. Another reason for the choice of local orbitals is that the BO effect is effective only when the charge fluctuation is faithfully represented in the VB structures. This means that the ionic structures are really ionic and the covalent ones are really covalent. When the orbitals are not local, a formally ionic structure is in fact contaminated by covalent ones and can at best reflect some damped charge fluctuation. Moreover, since one uses the full set of the VB structures, allowing the orbitals to delocalize would create artificial redundancy in the VB structure set. It follows therefore that the choice of purely localized active orbitals is in fact not a restriction on the orbital optimization, but rather a way to ensure a correct procedure.

On the other hand, there is no conceptual problem in letting the inactive orbitals be delocalized. For example, either the local p_x lone pairs of F_2 (in **9–11**) or their doubly occupied bonding and antibonding combinations represent two lone pairs facing each other. Thus, qualitatively both representations keep the same physical picture of this four-electron interaction. However, in flexible basis sets, the delocalized representation has more degrees of freedom over the localized one, since the building block AOs of the bonding and antibonding combinations can be different, thereby leading to a slightly better description of the four electron interactions. Therefore, the delocalization of inactive orbitals will be used as one of the possible options in the BOVB method. Of course, using localized active orbitals and delocalized inactive ones is valid only if inactive/active orbital rotations are not allowed. Practical means to avoid such spurious rotations are described in Sect. 4.5.

3.4 BOVB levels

Several theoretical levels are conceivable within the BOVB framework. Initially, the inactive orbitals may or may not be allowed to delocalize over the whole molecule (vide supra). To distinguish the two options, a calculation with localized inactive orbitals will be labeled L, as opposed to the label D that will characterize delocalized inactive orbitals. The usefulness and physical meaning of this option will be discussed using examples.

Another optional improvement concerns the description of the ionic VB structures. At the simplest level, the active ionic orbital is just a unique doubly occupied orbital as in **10** or **11**; however, this description can be improved by taking care of the radial correlation (also called "in–out" correlation) of the two active electrons, and this can be achieved most simply by splitting the active orbital into a pair of singly occupied orbitals

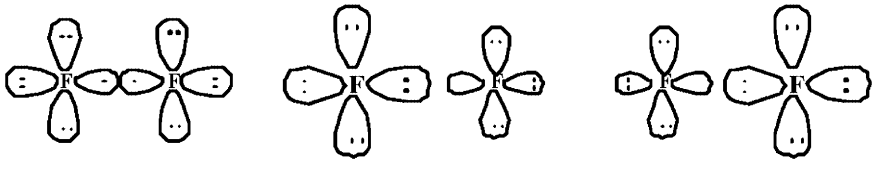

9 **10** **11**

Scheme 4

Table 1. Localized breathing-orbital valence bond (*L-BOVB*) calculation on the F_2 molecule at a fixed interatomic distance of 1.43 Å. The 6-31G* basis set was used. See Ref. [14] for more details

Iteration	Energy (au)[a]	D_e (kcal/mol)	Coefficients (weights)	
			Covalent **9**	Ionic **10** or **11**
0[b]	−198.71314	−4.6	0.840 (0.813)	0.194 (0.094)
1	−198.75952	24.6	0.772 (0.731)	0.249 (0.134)
2	−198.76494	27.9	0.754 (0.712)	0.258 (0.144)
3	−198.76572	28.4	0.751 (0.709)	0.260 (0.246)
4	−198.76600	28.5	0.752 (0.710)	0.259 (0.145)
5	−198.76608	28.6	0.750 (0.707)	0.261 (0.146)
Projected generalized valence bond[c]	−198.74554	15.7	(0.768)	(0.116)

[a] The Hartree–Fock bond energy is −33.4 kcal/mol at this interatomic distance
[b] Iterations 1–5 are BOVB calculations
[c] The valence bond weights are calculated after projecting the generalized valence bond wave function onto a basis of pure valence bond functions defined with strictly localized atomic orbitals

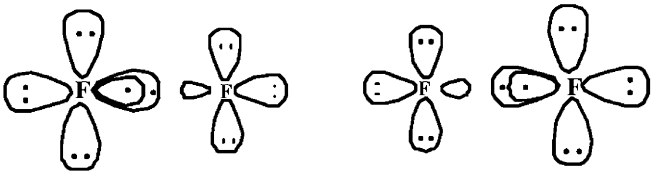

12 **13**

Scheme 5

accommodating a spin-pair, much as in GVB theory. This is represented pictorially in **12** and **13** (Scheme 5), which improve the descriptions of **10** and **11**.

This higher level will be referred to as S (for split), while the simpler unsplit level will carry no special label. Combining the two optional improvements, the BOVB calculations can be performed at the L, SL, D, or SD levels.[1] These levels were tested on bond energies and/or dissociation curves of classical test cases, representative of two-electron and odd-electron bonds.

4 Computational tests

4.1 The difluorine molecule

The dissociation of difluorine is a demanding test case used traditionally to benchmark new computational methods. In this regard, the complete failure of the Hartree–Fock method to account for the F_2 bond has already been mentioned. The calculated energies of F_2 at a fixed distance of 1.43 Å, relative to the separated atoms, are displayed in Table 1. Note that at infinite distance, the ionic structures vanish from the wave function that is described by a pair of singlet-coupled neutral atoms and corresponds to the Hartree–Fock situation of the separated atoms.

Since extensive basis sets are required to reproduce properties of this molecule, and we are using only 6-31G*, we cannot expect to reproduce the experimental bond energy. Therefore the best bonding energy is taken as the estimated full CI value, which is in the region of 30 kcal/mol. The classical VB level, referred to in Table 1 as iteration 0, is a simple nonorthogonal CI between one covalent and two ionic structures, using the pure AOs of fluorine, optimized for the free atoms. As can be seen, the bond energy at this latter level is extremely poor (though exceedingly better than Hartree–Fock) and still negative. The GVB level, which nearly corresponds to the same VB calculations but with optimized orbitals (all VB structures sharing the same set of orbitals), is much better but still far from quantitative. However, as soon as the orbitals are allowed to adapt themselves to the individual VB structures (BOVB levels in entries 1–5), the bond energy increases and converges rapidly to a value close to the full CI estimation. Thus, the BO effect just corresponds to that increment of the dynamic electron correlation that vanishes as the bond is broken. This provides a clear picture for the physical meaning of the dynamic correlation associated with the single bond, which is nothing but the wave-like quality of the electron manifested as the instantaneous adaptation of the orbitals to the charge fluctuation of the two bonding electrons.

Table 1 displays also the weights of the covalent and ionic structures, as calculated by means of the popular Chirgwin–Coulson formula, thus emphasizing the imbalanced ionic/covalent ratio that characterizes low levels of calculation.[2] The classical VB calculation, with orbitals taken from the free atoms, greatly disfavors the ionic structures with a weight that is much too small when compared with the best calculation, entry 5. The GVB wave function (projected on the basis of VB functions defined with pure AOs), with its orbitals optimized for the bonded molecule, is a little better, but it still suffers from the mean-field constraint. Now, when full freedom is given to the ionic structures to have their own orbitals, different from the covalent ones, the ionic weights gradually

[1] The L, SL, and SD levels were referred to as levels I, II, and III in Ref. [13]

[2] The weight W_n of a VB structure V_n is calculated as $W_n = \sum_m C_n C_n S_{nm}$, where C_n and C_m are the coefficients of V_n and V_m in the wave function and S_{nm} is their overlap

increase after each iteration. This clearly supports the previously stated intuitive proposal that the lack of dynamic correlation, which characterizes the classical VB, VBSCF, GVB, SC, or valence–CASSCF levels, results in an imbalance in the treatment of covalent versus ionic situations, and disfavors the latter structures.

The best calculation [14] corresponds to the simplest level of the BOVB method, referred to as L-BOVB. All orbitals, active and inactive, are strictly local, and the ionic structures are of closed-shell type, as represented in **10** and **11**. However the theory can be further improved, and the corresponding levels are displayed in Table 2. It appears that the L-BOVB/6-31 + G* level, yields a fair bonding energy, but an equilibrium distance that is rather too long compared to sophisticated estimations. This is the sign of an incomplete description of the bond. Indeed this simpler level does not fully account for the correlation of the active electrons, which are located in doubly occupied orbitals in the closed-shell ionic structures **10** and **11**. Splitting the active orbitals of the ionic structures as in **12** and **13**, i.e., the SL-BOVB level, remedies the deficiency. The corresponding SL-BOVB level displays an increased bonding energy and a shortened bond length compared to L-BOVB in Table 2.

The optimized equilibrium distance is still too long, however, and now the interactions between inactive electrons have to be considered. In the F_2 case, the inactive electrons involve the three lone pairs on each atom, facing each other. While their local AO or delocalized MO descriptions would be strictly equivalent in a minimal basis set, this is not the situation in more flexible basis sets. In a flexible basis set, the delocalized MO description implicitly allows some charge transfer from one lone pair of an atom to some outer-valence orbitals of the other atom [43]. Most of this charge transfer corresponds to some back-donation in the ionic structures, i.e., the fragment F^- that has an electron excess in its σ orbitals donates back some charge to the F^+ fragment through its π orbitals. Indeed, allowing the π lone pairs to delocalize (SD-BOVB entries in Table 2) results in a significantly shortened calculated bond length which is now in the expected range.

For the sake of comparison, Table 2 also displays some full CI estimations by Laidig, et al. [40], along with SD-BOVB calculations using the same basis set. The BOVB bonding distance appears perfectly correct, and the bonding energy seems to be within an acceptable margin of the full CI.

Table 2. Dissociation energies and optimized equilibrium bond lengths for the F_2 molecule calculated using different methods: generalized valence bond (*GVB*); valence bond self-consistent field (*VBSCF*); complete-active-space self-consistent field (*CASSCF*); L-BOVB; split, localized BOVB (*SL-BOVB*); split, delocalized BOVB (*SD-BOVB*); estimated full configuration interaction (*CI*)

Method	R_{eq} (Å)	D_e (kcal/mol)	Reference
6-31 + G* basis set			
GVB	1.506	14.0	[15]
VBSCF	1.551	10.6	This work
CASSCF	1.495	16.4	[15]
L-BOVB	1.485	27.9	[15]
SL-BOVB	1.473	31.4	[15]
SD-BOVB	1.449	33.9	[15]
Estimated full CI		< 33	[34]
Dunning–Huzinaga basis set[a]			
SD-BOVB	1.443	31.6	[15]
Estimated full CI	1.44 ± 0.005	28–31	[40, 41]
Experimental	1.412	38.3	[42]

[a] A modified Dunning–Huzinaga basis set used by Laidig et al. [40]. The normal (4,1) p contraction is extended to (3,1,1) and a set of six d functions of exponent 1.58 is added

4.2 The hydrogen fluoride molecule

Hydrogen fluoride is another classical test case, representing a typical polar bond between two atoms of very different electronegativities. As such, the molecule is expected to possess one ionic structure, F^-H^+, that is nearly as important as the covalent one. Thus, any deficiency in the description of ionic structures should result in significant error in the bonding energy and dissociation curve. Another distinctive feature of the F–H bond is its very high experimental bonding energy of 141 kcal/mol. With such strength of the bonding, one may wonder if the inactive electrons play the role assumed by the basic hypothesis of the BOVB method. For these two reasons, hydrogen fluoride is a challenging case, especially when the BOVB method can be assessed vis-à-vis benchmark full CI calculations that are available for the bond energy and the full dissociation curve.

The F^+H^- structure is expected to be very minor but is nevertheless added for completeness. The optimal bond lengths and bonding energies calculated at various theoretical levels, in the 6-31 + G** basis set and in an additional basis set comparable in quality to the one used by Bauschlicher and Taylor [44], are displayed in Table 3. Dynamic electron correlation effects appear once again to be an important component of the bonding energy, as evidenced by the GVB/6-31 + G** calculation yielding a value of only 113 kcal/mol, quite far from the experimental value. However the simple L-BOVB level also proves to be insufficient, with a bonding energy that is still too low. This is expected (vide supra), owing to the importance of the F^-H^+ ionic structure that is rather poorly described without splitting the doubly occupied orbitals. Splitting the active orbital of this structure, as we did for the ionic structures of F_2, leads to a spectacular improvement in the bonding energy, by about 12 kcal/mol (SL-BOVB/6-31 + G** entry in Table 3). As in the F_2 case, further improvement is gained by delocalizing the π inactive orbitals to reach the SD level that yields a bonding energy of 136.3 kcal/mol, in very reasonable agreement with the experimental value. A comparison of a full CI calculation by Bauschlicher and Taylor [44] with the SD-BOVB level using a common basis set is also displayed in Table 3.

By nature, the BOVB method describes properly the dissociation process. As a test case, the dissociation curve of the FH molecule was calculated at the highest BOVB level and compared with a reference full CI dissociation curve calculated by Bauschlicher et al. [45]

Table 3. Dissociation energies and optimized equilibrium bond lengths for the FH molecule

Method	R_{eq} (Å)	D_e (kcal/mol)	Reference
6-31 + G** basis set			
GVB(1/2)	0.920	113.4	[15]
L-BOVB	0.918	121.4	[15]
SL-BOVB	0.911	133.5	[15]
SD-BOVB	0.906	136.3	[15]
Bauschlicher–Taylor basis set[a]			
SD-BOVB	0.906	136.5	[15]
Full CI [b]	0.921	136.3	[44]
Experimental	0.917	141.1	[42]

[a] A double-zeta plus polarization plus diffuse basis set used by Bauschlicher and Taylor [44]
[b] The 2*s* orbitals are not included in the CI

with nearly the same basis set. The two curves, which were compared in Ref. [15], were found to be practically indistinguishable within an error margin of 0.8 kcal/mol, showing the ability of the BOVB method to describe the bonding interaction equally well at any interatomic distance from equilibrium all the way to infinite separation [15].

4.3 First-row transition-metal hydride cations

Bonds that involve transition metals are difficult to handle computationally, owing to two factors: the reshuffle of electronic configurations that accompanies the dissociation and the presence of a large number of inactive electrons that exert a great influence on the bonding electrons. In this context, previous theoretical studies of transition-metal hydride cations (TMH^+) showed that accurate predictions of bond dissociation energies require extended wave functions, which account for both static and dynamic electron correlation effects [46, 47]. Schilling et al. [46] showed that the GVB function by itself is unable to provide quantitative accuracy, but it predicts correct trends and elucidates the bonding patterns in first-row TMH^+. The factors which determine the bonding patterns [47] are the promotion energy of the metal cation from the $3d^{n+1}$ state to the bond-forming $4s^1 3d^n$ state, the loss of exchange in the $4s^1 3d^n$ state following bond formation, and the ground-state symmetry determined by the electrostatic repulsion between the *d* electrons. It is apparent therefore that VB theory is capable of providing very useful insight into bonding because it involves a compact, easily interpretable wave function. Further insight can be gained by employing the BOVB method that uses explicit covalent and ionic structures and can provide bonding patterns in terms of covalency, covalent–ionic resonance energy, and orbital relaxation of the $3d^n$ and $3s^2 3p^6$ shell electrons. Can the BOVB wave function, despite its extreme simplicity, still provide reasonable bonding energies in such difficult cases?

To answer this question, Galbraith et al. [48] used the BOVB method to study the bond energies of TMH^+ species (TM = Sc, Ti, V, Cr, Mn, Fe, Co, Ni, Cu, and Zn). The basis set involved a relativistic effective core potential for the $1s^2 2s^2 2p^6$ core and a triple-ζ (8s,7p,6d// 6s,5p,3d) basis for the 3*s*, 3*p*, 3*d*, and 4*s* shells of the metal, augmented with an f-type polarization function. For hydrogen, the triple-ζ (5s//3s) basis of Dunning was augmented with a p-type polarization function. At the dissociation limit, the BOVB wave function correlates with the restricted open-shell Hartree–Fock (ROHF) states of TM^+ and H. This level treats poorly the atomic states and especially the $3d^{n+1}$state. To correct for this non-VB-related deficiency, Galbraith et al. [48] used the technique recommended by Schilling et al. [46], Ohanessian and Goddard [47], and Petterson et al. [49] of shifting the energies of the TM^+ fragment using experimental data. Thus, the TMH^+ species are first dissociated into the atomic state most closely resembling their situation in the molecule (i.e., the $4s^1 3d^n$ state for TM^+), and whenever necessary, the experimental atomic state splitting is used to correct the energy of the TM^+ fragment to the corresponding atomic ground state.

The bond dissociation energies, calculated at the various computational levels, are displayed in Table 4 and are compared with experimental values. The VBSCF results are seen to be slightly better than the GVB results. Both results qualitatively reproduce the characteristic zigzag pattern of the experimental trends across the first transition metal row; however these two sets of bond energies are systematically too low, by 10–20 and sometimes by more than 30 kcal/mol, thus projecting the importance of dynamic correlation. Accordingly, a significant improvement is found upon moving from GVB or VBSCF to L-BOVB. The added flexibility of the BOVB method is seen to bring the predicted bond dissociation energies closer to the benchmark CCSD(T) values and to experimental results. Thus, while the VBSCF method (as well as the GVB or SC methods) captures the essential nondynamic correlation effects due to the bonding event, the BOVB method retains this qualitative picture, but adds the dynamic relaxation of all the electrons in response to bond pairing.

Still, the BOVB bonding energy for CuH^+ remains too small, by about 10 kcal/mol, an unusually large error for this method. However, CuH^+ is a particularly difficult case as can be judged by the VBSCF and GVB

Table 4. Bond dissociation energies (kcal/mol) of TMH^+ species, at the GVB, VBSCF, L-BOVB and CCSD(T) levels. The *M*–H bond lengths are optimized at the VBSCF level

	GVB	VBSCF	L-BOVB	CCSD(T)	Experimental[a]
ScH^+	47.4	46.4	57.5	55.2	57 ± 2
TiH^+	43.4	44.2	54.3	54.6	54 ± 3
VH^+	33.8	41.6	53.1	48.0	48 ± 2
CrH^+	8.9	9.5	26.1	37.3	32 ± 2
MnH^+	25.9	30.6	44.0	44.2	48 ± 3
FeH^+	31.2	36.0	53.9	51.9	50 ± 2
CoH^+	21.3	27.2	48.8	39.5	47 ± 2
NiH^+	9.7	16.1	40.3	39.3	40 ± 2
CuH^+	−22.2	−16.3	11.4	24.4	22 ± 3
ZnH^+	46.5	46.2	55.7	56.0	55 ± 3

[a] Experimental bonding energies from Ref. [75]

values, which are in error by 38 and 44 kcal/mol, respectively. Another source of inaccuracy comes from the use of VBSCF-optimized bond lengths, which were found to be generally too long by an average of 0.09 Å at this crude level [48]. Moreover, the BOVB calculation was limited to the simplest L-BOVB. It would be interesting to test the SD-BOVB level on these systems, with proper geometry optimization, to make a more critical evaluation of this unusual case.

4.4 Odd-electron bonds

Alongside electron-pair bonds, odd-electron bonds play an important role in chemistry, and constitute therefore a compulsory test case for any computational method. Odd-electron bonds can be represented as two resonating Lewis structures that are mutually related by charge transfer, as shown in Eq. 8 for two-center, one-electron bonds and in Eqs. (9) and (10) for typical two-center, three-electron bonds.

$$A \cdot B^+ \leftrightarrow A^+ \cdot B \tag{8}$$

$$A \cdot^+ : B \leftrightarrow A : \cdot B^+ \tag{9}$$

$$A \cdot : B^- \leftrightarrow A :^- \cdot B \tag{10}$$

According to qualitative VB theory, such bonds owe their strength to the resonance energy associated with the mixing of the two limiting structures. In MO theory the stability of these bonds is understood by inspection of orbital interaction diagrams **14** and **15** (Scheme 6), where σ and σ^* are bonding and antibonding combinations, respectively, of the active orbitals χ_a and χ_b of the fragments. Both diagrams display one net bonding electron. These diagrams can be further considered to question whether left–right electron correlation is still important in these odd-electron bonds. In **14**, the active space reduces to a single electron, and this eliminates the need for electron correlation within this space. On the other hand, the active space of **15** involves three electrons, and the only configuration that one might have added to possibly improve the simple Hartree–Fock wave function is $\sigma^1\sigma^{*2}$. This singly excited configuration does not mix, however, with $\sigma^2\sigma^{*1}$, by virtue of Brillouin's theorem. It follows that the concept of left–right correlation is meaningless in such systems, and that the description of both one-electron and three-electron bonds is already qualitatively correct at the Hartree–Fock level, in contrast to two-electron bonds, where this Coulomb correlation is important.

In view of the preceding conclusion, the failure of Hartree–Fock ab initio calculations to reproduce three-electron bonding energies might seem to be a paradox. Clark [50] and Gill and Radom [51] carried out systematic calculations on a series of cation radicals involving three-electron bonds between atoms of the second and third rows of the periodic table, and showed that the Hartree–Fock error is always large, sometimes of the same order of magnitude as the bonding energy itself. Focusing on the three-electron case, the puzzling Hartree–Fock deficiency can be analyzed by expanding the corresponding wave function into its VB constituents, as we did in the two-electron case. Taking the F_2^- case as an example, the Hartree–Fock wave function Ψ_{HF} (3*e*) reads

$$\Psi_{HF}(3e) = |\ldots \varphi_i \ldots \sigma\bar{\sigma}\sigma*| \ , \tag{11}$$

where φ_i represent the inactive orbitals, and the active orbitals σ and σ^* are defined as in **14** and **15**. Expanding σ and σ^* (dropping the normalization constants) leads to Eq. (12):

$$\Psi_{HF}(3e) = |\ldots \varphi_i \ldots \chi_a\bar{\chi}_a\chi_b| + |\ldots \varphi_i \ldots \chi_a\bar{\chi}_b\chi_b| \ . \tag{12}$$

Thus, the Hartree–Fock wave function is equivalent to a two-configuration VB wave function. The same VB structures, **16** and **17** (Scheme 7), were in fact used in the original VB treatment of three-electron bonds by Pauling [52].

Even though physically correct, the ROHF wave function suffers from the same defect as the GVB or the VBSCF wave function for two-electron bonds. Thus, the active AOs are common for the two structures and are not adapted to their instantaneous occupancies, while the inactive orbitals are not adapted to the instantaneous charge of the fragments. Once again, this defect can be removed by use of the BOVB wave function, which allows different orbitals for different structures, as in Eq. (13):

$$\begin{aligned} \Psi_{BOVB}(3e) \ = \ & C_1|\ldots \varphi_i \ \ldots L_a\bar{L}_aR_r| \\ & + C_2|\ldots \varphi_i' \ \ldots L_r\bar{R}_aR_a|, \\ & L_a \neq L_r;\ R_r \neq R_a;\ \varphi_i \neq \varphi_i' \ . \end{aligned} \tag{13}$$

Here the orbitals are defined in the same way as in Eqs. (5), (6), and (7).

Let us now turn to actual BOVB computation of the F_2^- anion, as an archetype of three-electron-bonded radicals. As is the case for its neutral homologue, the difluorine radical anion is a difficult test case for the calculation of the bonding energy. At the Hartree–Fock level, the bonding energy is about ± 4 kcal/mol, depending on whether the ROHF or the unrestricted Hartree–Fock method is used. The experimental bond energy is 30 kcal/mol. In contrast, the second-order Møller–Plesset (MP2) and fourth-order Møller–Plesset (MP4) methods are successful, and this success emphasizes the dynamic nature of electron correlation for this molecule.

The computed equilibrium distance and bonding energy of F_2^- are displayed in Table 5. To appreciate better the sensitivity of active versus inactive orbitals to the BO

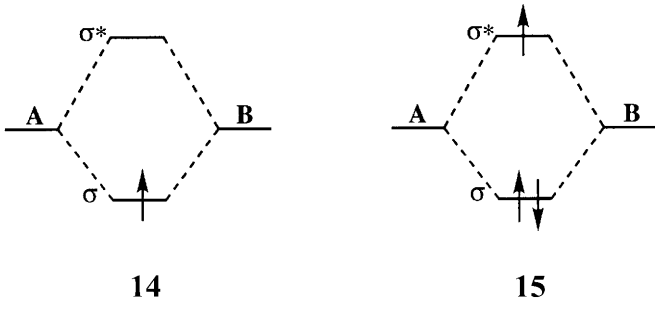

14 **15**

Scheme 6

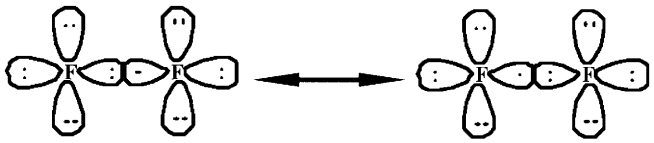

16 **17**

Scheme 7

Table 5. Calculated equilibrium distances and dissociation energies for the F_2^- radical anion, (6-31 + G* basis set). The BOVB calculations were performed with all valence orbitals being included in the set of breathing orbitals (fully breathing option) unless otherwise specified (entry 2)

Entry method		R_{eq} (Å)	D_e (kcal/mol)	Reference
1	ROHF		−4	[34]
2	L-BOVB (active set only)	1.954	13.3	
3	L-BOVB	1.964	29.7	[16]
4	D-BOVB	1.954	30.1	
5	SD-BOVB	1.975	28.0	
7	MP2	1.916	26.2	[16]
8	PMP2	1.935	29.5	
9	MP4	1.931	25.8	[53]
10	Experiment		30.2	[42]

effect, the latter was introduced in steps. In the first step no BOs are used ($L_a = L_r$, $R_a = R_r$, $\varphi_i = \varphi_i'$). This VBSCF calculation is nearly equivalent to the ROHF level. In the second step, only active orbitals are included in the breathing set ($L_a \neq L_r$, $R_a \neq R_r$), while in the next step full breathing is permitted ($L_a \neq L_r$, $R_a \neq R_r$, $\varphi_i \neq \varphi_i'$). The latter wave function, at the L-BOVB level, can be represented as in **18** and **19** (Scheme 8).

The BO effect, restricted to the active orbitals that are directly involved in the three-electron bond, already improves the bonding energy by some 17 kcal/mol relative to the ROHF value (Table 5). Extension of the BO effect to the inactive orbitals brings another 16 kcal/mol, yielding a final bonding energy of 29.7 kcal/mol, in excellent agreement with the experimental bonding energy of 30.2 kcal/mol [42].

The Hartree–Fock error is thus completely corrected by the BO effect. On a "per orbital" basis, each active AO contributes 8.6 kcal/mol to the overall BO stabilization, while the inactive lone pairs have a lesser influence, about 2.8 kcal/mol each. It is seen that increasing the level of theory from L- to D- or SD-BOVB does not change much the calculated bonding energy, indicating that the fully localized AOs are, right at the outset, well adapted to the description of the three-electron interaction, in contrast to the situation in two-electron bonds.

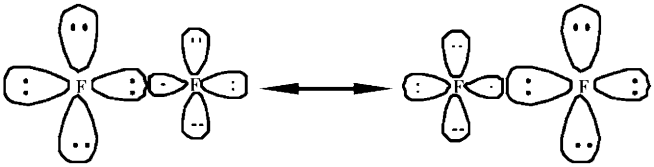

18 **19**

Scheme 8

The performances of the various BOVB levels can be compared to those of Møller–Plesset (MP) perturbation theory, yet with some caution since the various MP orders do not converge well. This is due to a rather large spin contamination at the unrestricted MP2 level, which leads to a wave function with an $\langle S^2 \rangle$ value of 0.78. Keeping in mind that the breathing orbitals of F_2^- are not very polarized [16], the bonding energy is not expected to be very basis set dependent, so the SD-BOVB value of 28.0 kcal/mol is entirely reasonable relative to the experimental value of 30.2 kcal/mol. The BOVB calculated equilibrium bond lengths are rather long relative to the values calculated at the various MP levels (no experimental value is available), and both sets of values display significant variations from one level to the other. This inaccuracy is, however, normal, owing to the extreme flatness of the potential surface near the energy minimum. Indeed, at the MP4 level the force constant is only 0.55 mdyn/Å, which means that stretching the bond by 0.02 Å away from equilibrium results in an energy rise of only 0.03 kcal/mol.

A final point concerns the avoidance of symmetry-breaking artefacts by BOVB as opposed to other methods. Three-electron bonds, just like any electronic system that must be described by more than one Lewis structure, are subject to the symmetry-breaking artefact with most computational methods based on MOs: Hartree–Fock, MP2, or MP4, and even CCSD and CCSD(T) [54, 55]. This symmetry-breaking is observed beyond a critical interatomic distance, which may actually happen to be shorter than the equilibrium bond length, and it is due to competition, during orbital optimization, between the resonance effect and the BO effect (called "size effect" by other authors [56, 57] in this case). Assuming, for example, that the orbital optimization is performed at the Hartree–Fock level, the wave function is subject to the so-called "symmetry dilemma": that is, if the symmetry of the wave function is broken, it converges to a solution like **18** alone, in which the orbitals are adapted to their occupancy but where the resonance is lost. On the other hand, if the symmetry is maintained, the wave function converges to a solution of the type **16** ↔ **17**; this benefits from the resonance energy, but the orbitals are optimized in a mean field, and are consequently poorly adapted to their instantaneous occupancy. In cases where the resonance is dominant, the wave function displays the correct symmetry. However, as soon as the resonance becomes too weak to overcome the BO effect, the wave function departs from the molecular symmetry and leads to unphysical geometries, frequencies, and energetics. This problem, which is rather difficult to overcome with standard computational methods, vanishes at the BOVB level: as the wave function involves both the size effect and the resonance effect at any molecular geometry, the root cause for the symmetry-breaking disappears. The BOVB method is, by nature, free from the symmetry-breaking artefact.

4.5 General procedure for low-symmetry cases

Up to this point we have dealt with molecules with high symmetry that helps the distinction between active and inactive orbitals. Such symmetry is not always present in the general case, and this poses a danger that during the BOVB orbital optimization, some flipping will occur between the sets of active and inactive orbitals.

The simplest level, L-BOVB, presents no particular practical problem. Fast convergence is generally obtained by using well-adapted guess orbitals, which can be chosen as the Hartree–Fock orbitals of the isolated fragments with the appropriate electronic charge. Thus, the guess orbitals for the covalent structure are those of the isolated radicals, while the orbitals of the isolated anions and cations can be taken for the ionic structures.

Moving to the more accurate SL-BOVB level merely requires checking that the orbital being split (in an ionic structure) is indeed an active orbital and does not end up belonging to the inactive space after the optimization process. While this condition is generally met by choosing an appropriate guess function in high-symmetry cases (F_2 or HF earlier), in the general case nothing guarantees a priori that this exchange between the active and inactive spaces will not take place, leading for example to **20** instead of the correct structure **21** in the case of $H_2N{-}NH_2$ (Scheme 9).

To circumvent this difficulty, a general procedure was developed. After the L-BOVB step, the orbitals are initially subject to localization using any standard method, then the active orbitals are split while the inactive ones are kept frozen during the optimization process.[3]

Delocalization of the inactive orbitals (D-BOVB or SD-BOVB) is important for getting accurate energetics. Once again, it is important to make sure that the orbitals that are delocalized are the inactive ones, while the active set remains purely localized, which is the basic tenet of the method. Otherwise, any number of artefactual solutions might be found. To avoid a spurious exchange between the active and inactive spaces during the orbital optimization process, it is possible to start from an L-BOVB or SL-BOVB wave function, then allowing delocalization of the inactive orbitals while freezing, this time, the active orbitals during the subsequent optimization process that leads to the D-BOVB or SD-BOVB levels, respectively.

Some computational tests of the general method, which were applied to highly symmetric molecules as well (e.g., F_2) for consistency, are displayed in Table 6. The bonding energies, calculated after geometry optimization at the MP2 level in the same basis set as the BOVB calculations, are directly compared to experiment. It is seen that the SD-BOVB computed bonding energies are all close to the experimental values, despite the modest size of the basis set, and this deserves some comment. First, let us note that the bonding energy for F_2 is slightly larger than the value that is reported in Table 2. This is due in part to the 6-31G* basis set, which yields slightly larger bonding energies (with any computational method) than

[3]This requires prior orthogonalization of the orbitals within each fragment

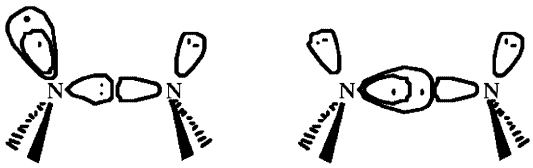

20 **21**

Scheme 9

Table 6. Some BOVB-calculated bonding energies in double-zeta polarized basis sets

	BOVB level	Basis set	D_e (theory)	D_e (exp)[a]
$H_3C{-}H$	SD	6-31G**	105.7	110.3[a]
$H_3C{-}CH_3$	SD	6-31G*	94.7	96.8 ± 0.3[b]
$H_2N{-}NH_2$	SD	6-31G*	68.5	72.6 ± 2.0[b]
HO–OH	SD	6-31G*	50.8	54.6[c]
F–F	SD	6-31G*	36.2	38.3

[a] See Ref. [61]
[b] Ref. [76]
[b] Experimental D_0 cited in Ref. [77]
[c] Zero-point-energy (*ZPE*) correction from experimental IR frequencies found in Ref. [78]
[d] Ref. [42]

basis sets involving diffuse orbitals. The other reason is that with the general procedure, the 2*s* inactive orbitals of each fluorine atom are also allowed to delocalize at the SD level, whereas in Table 2 only the π inactive orbitals, which alone could be distinguished from active ones by a symmetry criterion, were allowed to delocalize. As a result, the bonding energies of F_2 and the other molecules displayed in Table 2 are consistently closer to experiment than to the expected full CI estimation in the same basis set, and this emphasizes the systematic tendency of the SD-BOVB level, which can be understood by considering the nondynamic correlation of the inactive electrons. Normally, these electrons are left uncorrelated in the molecule as well as in the dissociated fragments or in any conformation of a molecular system throughout a potential surface; however, since the inactive orbitals are somewhat different in the HL and ionic VB structures, it is impossible to avoid the fact that such a difference in a multistructure wave function will bring in some nondynamic correlation of the inactive electrons. This is a rather fortunate systematic error, since generally the basis set that is used is far from complete and the slight BOVB overbinding compensates for the basis set deficiency.

4.6 Summary of the computational tests

The generally good performance demonstrates that the BOVB wave function, despite its very small size, captures the essence of the chemical bond, be it of the odd-electron or of the two-electron type, polar as well as nonpolar. The complete neglect of Coulomb correlation

within the inactive space has no significant consequences for the relative energies. This in turn means that the inactive electrons require dynamic correlation, associated with the fact that their orbitals undergo changes in size, polarization or hybridization. However, these electrons have some nearly constant Coulomb correlation energy. In fact, just the bare minimum electron correlation is taken into account since the method becomes equivalent to a Hartree–Fock calculation of the separated fragments at the dissociation limit. Thus, the method calculates only the differential electron correlation, which involves the left–right electron correlation of the active electrons, and the dynamic correlation associated with the formation of the bonds. Since the latter term is nascent from the instantaneous adaptation of the orbitals to the charge fluctuation of the active electrons, dynamic correlation effects are particularly important in three-electron bonds, because in such systems the stabilizing interaction originates only in the charge fluctuation between the two VB structures.

While all BOVB levels provide nearly equally good bonding energies for the three-electron bonds, the same does not hold true for two-electron bonds, which often require the best levels for an accurate description. Splitting the active orbitals in the ionic structures is important when the bond is polar. Moreover, the interatomic interactions between inactive orbitals are important in two-electron bonds, owing to their short equilibrium bond lengths. Such interactions are adequately taken into account by delocalizing the inactive orbitals.

Finally, a few remarks are in order concerning the nondynamic correlation of the inactive electrons. As already pointed out, a small part of this correlation is taken into account in the molecule but not in the separated fragments, and this systematic artefact has the effect of deepening the potential well, thus compensating for the small size of the basis sets that are usually used. Now one may wonder if the use of large basis sets would lead to BOVB bonding energies which would be significantly larger than experimental ones. Our experience shows that in all the examples we have tested this is not the case. The main effect of using a large basis set in standard MO ab initio calculations is that it permits angular correlation to be taken into account. This type of electron correlation is associated with double electronic excitations towards high-rank polarization orbitals, and such excitations are not normally present in a compact BOVB wave function as defined earlier. It follows that using large basis sets in the BOVB framework is of course possible, but should not lead to overly large bonding energies.

However, some cases may be imagined in which this spurious correlation of the inactive electron would replace the BO effect of the active electrons, leading to nonsensical bond energies. This might happen, for example, if the active orbitals were allowed to delocalize freely as in the GVB method. The outcome might be that the active orbitals are all the same in the HL and ionic structures, being of CF type, thus representing a triplicate active system of GVB type. On the other hand, the degree of freedom of the BOVB wave function would be used to make the inactive orbitals very different from each other in the three structures, so the resulting wave function would display some correlated inactive electrons. This would bring an additional correlation effect that stabilizes only the molecule but not the fragments because, at the asymptotic geometry, the HL structure is the only VB configuration that remains. This stresses the importance of keeping the active orbitals as strictly localized on their respective atom or fragment. A BOVB calculation would become meaningless if the active orbitals were freely allowed to delocalize. Other caveats were discussed in the literature [48].

5 Diabatic states

One of the most valuable features of theoretical methods based on classical VB structures is their ability to calculate the energy of a diabatic state. For a recent method of generating diabatic and adiabatic states using VB-type concept within molecular mechanical formulation see Ref. [58]. For practical applications, some diabatic bond energy curves of chemical interest can be, for example, the separate dissociation energy curves of the ionic and covalent components of a bond, or the energy curves of the effective VB structures of a chemical reaction which are traced individually along a reaction coordinate. Such diabatic curves are plotted in the curve-crossing VB diagrams which are used to predict and interpret reaction barriers [5, 6]. Diabatic states have also some applications related to the concepts of organic chemistry, like resonance energy.

5.1 Definition

While the definition of an adiabatic state is straightforward, as an eigenfunction of the Hamiltonian within the complete set of VB structures, the concept of diabatic state is less clear-cut and accepts different definitions. Strictly speaking, a basis of diabatic states (ϑ, ϑ'...) should be such that Eq. (14) is satisfied for any variation, ∂Q of the geometrical coordinates.

$$\langle \vartheta | \partial / \partial \mathrm{Q} | \vartheta' \rangle = 0 \tag{14}$$

However this condition is impossible to fulfill in the general case with more than one geometrical degree of freedom, so one has to search for a compromise in the form of a function whose physical meaning remains as constant as possible along a reaction coordinate. Clearly, a single VB structure that keeps the same bonding scheme irrespective of the geometry of the system is the choice definition for a general diabatic state [59]. For example, if we consider the A–B molecule in the BOVB framework, the ground state (made of three VB structures) will be adiabatic, while the three VB structures, A–B, A^+B^- and A^-B^+, will be the diabatic states. Note, however, that a given diabatic state can generally correspond to a mixture of VB structures representing a given Lewis bond. For instance, in the S_N2 reaction (Eq. 4), one diabatic state could be the bonding scheme of the reactants, $Cl^- + H_3C\text{-}F$, while the other would

represent the products, $Cl{-}CH_3 + F^-$. In this case, each diabatic state would be made of three VB structures, **3**, **5**, **6** and **4**, **5**, **7**, corresponding to the covalent and two ionic components of the carbon–halogen bond. Such diabatic states constitute the crossing curves of the VB correlation diagrams of Shaik and Pross [5, 6].

5.2 Practical calculations

Having defined a diabatic state as a unique VB structure, or more generally as a linear combination of a subset of VB structures, in the next step one has to specify the orbitals needed to construct the VB structure(s) of this diabatic state. An initial possibility is to keep for the diabatic state the same orbitals that optimize the adiabatic state, something that has the advantage of simplicity. In practice, this can be achieved as follows. Once the orbitals have been determined at the end of the BOVB orbital optimization process, the Hamiltonian matrix is constructed in the space of the VB structures and the adiabatic energies are calculated by diagonalization of the Hamiltonian matrix. The energies of the diabatic states are just the respective diagonal matrix elements.

A problem with this diabatization procedure is that it does not guarantee the best possible orbitals for the diabatic states. Indeed, the BOVB orbitals are optimized so as to minimize the energy of the multistructure ground state and are therefore the best compromise between the need to lower the energies of the individual VB structures and to maximize the resonance energy between these VB structures. This latter requirement implies that the final orbitals are not the best possible orbitals to minimize each of the individual VB structures taken separately. It follows that the diabatic states calculated in this way may appear surprisingly high in energy. For instance, the purely covalent $H_3C{-}Cl$ bond appears to be repulsive, if calculated this way, which is unreasonable.

An alternative approach, which we recommend, consists of optimizing each diabatic state separately, in an independent calculation. As a result, the resulting orbitals of the diabatic states are different from those of the adiabatic states, and each diabatic state possesses its best possible set of orbitals. The diabatic energies are obviously lower compared with those obtained by the previous method. Using again the $H_3C{-}Cl$ bond as an example, this second procedure now yields an energy profile for the purely covalent structure, with a bonding energy of 34 kcal/mol, in agreement with common sense as opposed to the repulsive covalent interaction obtained in the first procedure. We therefore believe that the separate calculation of the diabatic states yields the best possible results in terms of chemical interpretation. It leads to variational adiabatic and diabatic states.

It might be argued that the diabatic states, calculated separately as we recommend, are subject to basis set dependency. Thus, in principle, in the limit of an infinite basis set, there would be so many and such diverse polarization functions that the optimized orbitals could not be considered anymore to be localized, so the diabatic state would converge to the ground state rather than to a specific VB structure. However, in practice, a few tests showed that as long as standard basis sets are used such basis set dependency remains marginal. As an example, adding a set of diffuse functions to the 6-311G* basis set was found in one of our applications to change the energy of the diabatic state by only 0.1–0.2 kcal/mol relative to the ground state [19].

5.3 Resonance energies

Many molecules are represented as a set of resonating structures. For example, the ground state of formamide is the optimized mixture of the VB structures **22** and **23** (Scheme 10). The resonance energy, which is responsible for the rotational barrier, is the energy difference between the major VB structure **22** and the ground state.

Thus, the resonance energy characterizes the insufficiency of structure **22** to represent the ground state. It is clear, therefore, that this concept is best quantified by comparing the energy of the optimized ground state with that of the best possible wave function for **22**, and this is meaningful only if the orbitals of the diabatic state that represents structure **22** are optimized for this specific state alone, as recommended earlier. Accordingly, the method for calculating resonance energies in the BOVB framework consists of separate optimizations of the ground state and of the major VB structure (the one that has the largest weight in the wave function). The resonance energy is the difference between the variational energies of the full state and the reference VB structure. In this manner the resonance energy itself is variational. Tests of these variational resonance energies show that they reproduce experimentally determined values, for example, for benzene and cyclobutadiene [60, 61].

6 Some applications of the BOVB method

Some applications of the BOVB method to effective chemical problems have already been made by various authors. Langenberg and Rutink [20] used the BOVB method as a means to solve the symmetry-breaking artefact in the potential-energy surface of the glyoxal cation. This property of the method was also exploited by Humbel et al. [21] in the investigation of the $H_2O_2^-$ potential surface. Basch et al. [22] applied the method to study the $SiH_3{-}F$ bond and to calculate the covalent versus ionic dissociation curves of $CH_3{-}Y$ molecules (Y = F, OH, NH_2, CH_3, BH_2, CN, NO) [23]. Calcula-

22 **23**

Scheme 10

tions of diabatic states were performed by Lauvergnat et al. to characterize the lone-pair bond-weakening effect in the H–NH_2, H–OH and H–F bonds [18]. The diabatic states were also used in the generation of VB curve-crossing diagrams for hydrogen-transfer reactions between X groups (X = H, CH_3, SiH_3, GeH_3, SnH_3, PbH_3) [24], and for identity radical-exchange reactions of the type $H + XH' \rightarrow HX + H'$ and $X + HX' \rightarrow XH + X'$ (X = F, Cl, Br). The covalent versus ionic nature of homonuclear and heteronuclear π bonds was investigated [19], and a new type of bonding, in which the strength of the bond is primarily due to an exceptional energy of resonance between the covalent and ionic forms, was discovered [19, 60, 61, 62]. Here, we focus on this latter application, which is typical of the insight the BOVB method can bring.

6.1 The nature of the C–Cl versus Si–Cl bonds

Bonding in first- versus higher-row atoms poses a number of interesting problems, among which is the curious reluctance of R_3Si–X bonds to heterolyze [63, 64, 65, 66, 67] in solution, in comparison with the ease of heterolysis in R_3C–X compounds. So rare are the $R_3Si^+X^-$ species in the condensed phase that a compound such as Ph_3SiClO_4 that appeared initially as an excellent candidate for an ionic bond was found to be a covalent solid exhibiting a Si–O bond [68]. In contrast, the carbon analog is definitely ionic, $Ph_3C^+ClO_4^-$ [69, 70]. It seems that Si has a very strong affinity for covalent interactions, much stronger indeed than carbon, and that it requires counterions such as hexabromocarborane to approach, even then not completely, an ion pair situation, $R_3Si^+X^-$ [71]. This difference between bonding at silicon and carbon cannot be explained by electronegativity considerations since silicon is much more electropositive than carbon and might as such be expected to be more prone to form free cations. Such intriguing experimental facts raise fundamental questions that require understanding, which can only be gained through a detailed investigation of the covalent and ionic interactions and their interplay in Si–X versus C–X bonds. The BOVB method is suitable for this purpose, and was used to study the model systems H_3Si–Cl and H_3C–Cl [62, 72]. We mention this study in some detail, since it demonstrates the insight that can be gained by the use of diabatic state curves to solve a chemical problem.

The adiabatic bond energies calculated at the SD-BOVB level, in the 6-31G* basis set, are compared in Table 7 to the experimental and G1 and G2 energies. The underestimation of the BOVB-estimated bonding energies relative to experiment is significant, 7.4 and 9.4 kcal/mol respectively for the C–Cl and Si–Cl bond, but in the expected range in view of the small basis set used in this semiquantitative study, much smaller than the basis set used at the G2 level [73, 74].

The dissociation curves representing the ground states, the purely covalent and lowest purely ionic curves of the two molecules are displayed in Figs. 1 and 2, respectively, as calculated at the SD-BOVB level. It is seen that in both molecules the covalent structure is bonded relative to the separate fragments by a significant amount. This bonding energy is the covalent contribu-

Table 7. Bond energies (kcal/mol) for H_3C–Cl and H_3Si–Cl at various levels

Species	Experiment[a]	SD-BOVB[b]	G1[c]	G2[c]
H_3CCl	87.3	79.9	88.9	88.3
H_3SiCl	110.7	101.7	111.9	110.7

[a] D_e obtained from experimental D_0 values quoted in Ref. [70] and corrected by a calculated ΔZPE from Ref. [74]
[b] Optimized geometric values [GVB(1/2)/6-31G*] are R_{CCl} = 1.815 Å, R_{CH} = 1.078 Å, ∠(HCCl) = 108.1°, R_{SiCl} = 2.086 Å, R_{SiH} = 1.468 Å, ∠(HSiCl) = 108.3°
[c] G1 and G2 values from Refs. [73, 74]

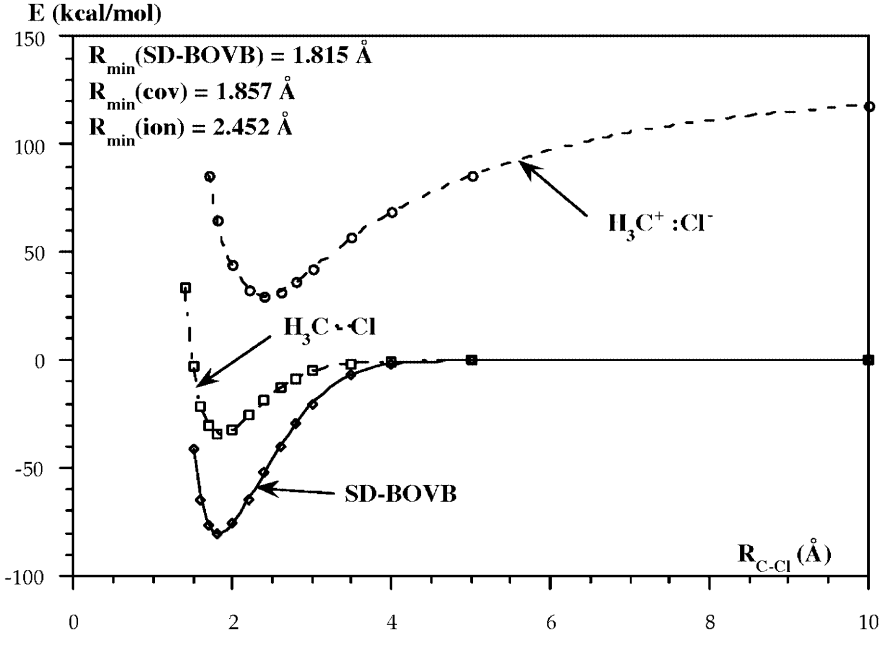

Fig. 1. Dissociation energy curves for the pure ionic ($H_3C^+Cl^-$) and the pure covalent (H_3C–Cl) structures, and the split, delocalized breathing-orbital valence bond (*SD-BOVB*) ground state for the H_3C–Cl bond

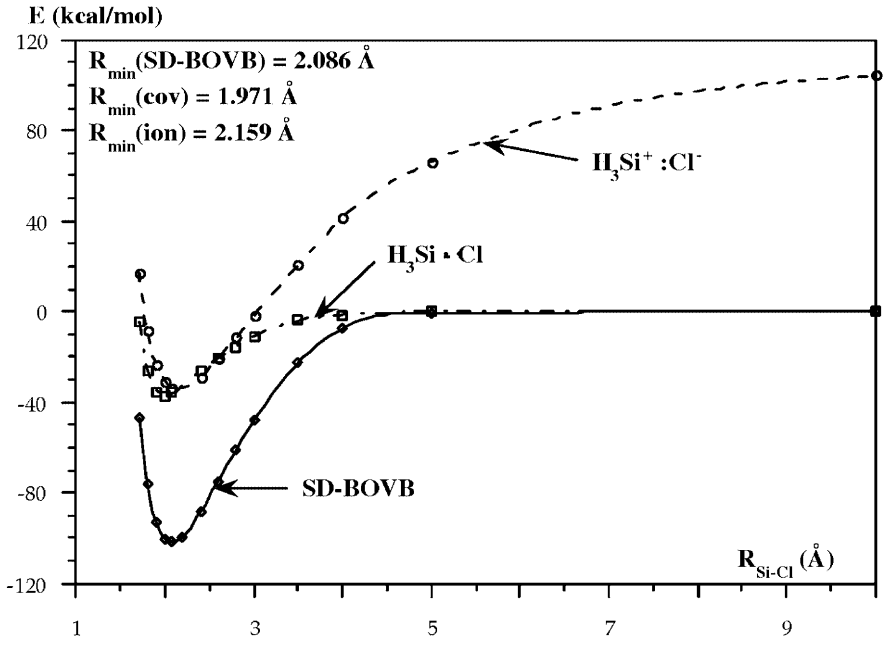

Fig. 2. Dissociation energy curves for the pure ionic ($H_3Si^+Cl^-$) and the pure covalent (H_3Si–Cl) structures, and the SD-BOVB ground state for the H_3Si–Cl bond

tion that arises solely from the spin-pairing of the two electrons, which are localized on their respective fragments. Interestingly, these covalent interaction energies are almost the same for both systems, 34 kcal/mol for H_3CCl and 37 kcal/mol for H_3SiCl. On the other hand, the optimal distance for the purely covalent bond is, expectedly, longer in the Si–Cl than in the C–Cl bond.

More surprising are the features of the ionic curves for the two molecules. While the minimum of the $H_3C^+Cl^-$ curve is located at a bonding distance of 2.452 Å, that of $H_3Si^+Cl^-$ is found at a significantly shorter distance, 2.159 Å. As such, the effective radius of the H_3Si^+ cation is smaller than that of H_3C^+, in the opposite order to the sizes of the silicon and carbon atoms. Moreover, the ionic potential well of $H_3Si^+Cl^-$ is much deeper than that of $H_3C^+Cl^-$, with an ionic bonding energy of 139 versus 89 kcal/mol, relative to the asymptotic values calculated at a separation of 10 Å between the ionic fragments. These different features of the $H_3Si^+Cl^-$ and $H_3C^+Cl^-$ ion pairs can be understood by considering the detailed net charges on both cations, as calculated [62, 72] by means of a natural bond orbital analysis. It appears that while the positive charge in the CH_3^+ cation is dispersed on all atoms, in the silicenium cation it is concentrated on the silicon atom. The calculated net charges amount to only 0.284 on carbon versus 1.464 on silicon in the two respective cations, as calculated at the same geometries they possess in the R_3M–Cl molecules [62, 72]. It is apparent, therefore, that $H_3Si^+Cl^-$ will possess a much stronger electrostatic interaction compared with $H_3C^+Cl^-$; hence the deeper potential-energy curve and the shorter optimal distance.

While the covalent curve is the lowest of the two diabatic curves in both molecules, the covalent–ionic energy gap is much larger in H_3C–Cl than in H_3Si–Cl, in the bonding regions, as expected from electronegativity considerations. Nevertheless, the interaction between covalent and ionic structures is very important in both cases. The formation of the ground-state bond at each point of the $R_{M...Cl}$ (M = C, Si) coordinate arises primarily from the mixing of the covalent VB structure with the lowest ionic structure, through an interaction matrix element which is the classical resonance integral β, defined over the bond hybrids. The resulting increase in the bond energy, relative to the covalent curve, is the covalent–ionic resonance energy.

Table 8. Weights and coefficients of covalent and ionic structures for H_3C–Cl and H_3Si–Cl at the SD-BOVB level

	Coefficients	Weights
H_3C–Cl	0.646	0.616
$H_3C^+Cl^-$	0.358	0.269
$H_3C^-Cl^+$	0.190	0.115
H_3Si–Cl	0.628	0.572
$H_3Si^+Cl^-$	0.522	0.459
$H_3Si^-Cl^+$	0.075	−0.031

Let us turn now our attention to the nature of the M–Cl bond at its equilibrium geometry. The coefficients of the covalent and ionic structures in the ground states of H_3SiCl and H_3CCl are displayed in Table 8, along with their calculated weights. At the SD-BOVB level, the C–Cl bond is described as mostly covalent, with a weight of about 62%, compared with a weight of 27% for the lowest ionic structure, C^+Cl^-, while the other ionic structure, C^-Cl^+, is marginal. On the other hand, the Si–Cl bond has rather similar covalent and ionic weights (57% and 46%, respectively), in agreement with the near degeneracy of the corresponding VB structures, at equilibrium bonding distance. The second ionic VB structure, Si^-Cl^+, is totally negligible, having a small negative weight, which in the Chirgwin–Coulson definition is interpreted as close to zero.

As may be seen from Figs. 1 and 2 the resonance energy is strikingly large, about 46 kcal/mol for CH_3Cl and about 66 kcal/mol for SiH_3Cl. In fact, in both cases the major bonding interaction that glues the two fragments is the resonance energy, and for the Si–Cl bond this contribution is truly dominant, being about 65% of the total bond energy. The reason for this qualitative difference between the C–Cl and Si–Cl bonds is the energy gap between the covalent and the major ionic structure $MH_3^+Cl^-$ that is significant in CH_3Cl but extremely small in SiH_3Cl. This difference is the consequence of three additive effects:

1. The lower ionization energy of $SiH_3^\bullet$ relative to $CH_3^\bullet$ globally lowers the $H_3Si^+Cl^-$ curve compared to that of $H_3C^+Cl^-$.
2. The deeper ionic potential well of $H_3Si^+Cl^-$ relative to $H_3C^+Cl^-$ (vide supra).
3. The coincidence of the ionic and covalent minima, on the dissociation coordinate, in the SiH_3Cl case, in contrast with the different ionic and covalent optimal distances in CH_3Cl.

How would these bonding features be modified in a polar solvent? Having a larger dipole moment, the ionic component of a covalent bond will be stabilized, by interacting with solvent molecules, relative to the covalent component [6, 13]. This differential stabilization is very large when at a large distance between the fragments, and gets smaller as the distance decreases. The consequence is that the ionic curve becomes flat, it crosses the covalent curve and defines an ionic dissociation limit. Why does this mechanism, which is well accepted for the C–X dissociation in R_3C–X, seem to be inefficient in the R_3Si–X case? While this problem must await a proper solvation treatment, the results have shed enough light on the natures of the C–Cl and Si–Cl bonds to suggest the working hypotheses depicted in Fig. 3.

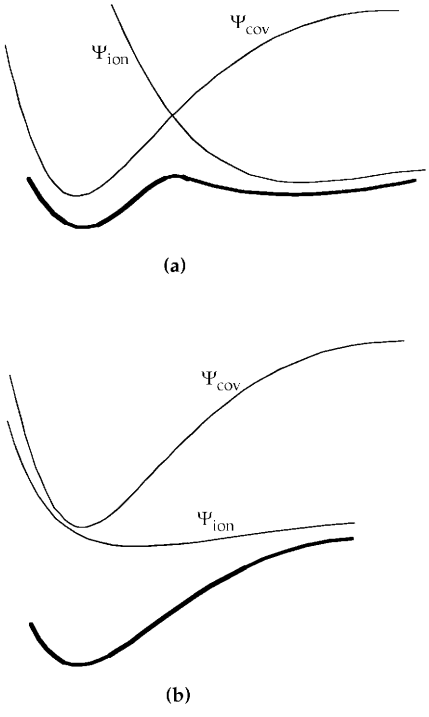

Fig. 3a,b. Schematic covalent (Ψ_{cov}) and major ionic (Ψ_{ion}) diabatic dissociation curves of an R_3M–X species in a polar solvent. The ground-state dissociation curve (*bold line*) results from the mixing of the diabatic curves Ψ_{cov} and Ψ_{ion}. **a** The R_3C–Cl case. **b** The R_3Si–Cl case

Figure 3a shows the situation in R_3C–X. This is a typical scenario of an efficient heterolytic cleavage. The ionic curve, Ψ_{ion}, retains its gas-phase minimum [13], which now becomes the minimum for the tight ion pair. At shorter distances the ionic structure rises in energy, crosses the covalent structure, Ψ_{cov}, and by avoided-crossing leads to a transition state for the heterolysis. In the R_3Si–X case, the ionic curve which was already close to the covalent one in the gas phase (see Fig. 2) now descends below the covalent curve but remains quite close since the solvation of $R_3Si^+X^-$ is not so favorable. Indeed, the net dipole of the $R_3Si^+X^-$ ionic structure should be quite small because the R_3Si^+ cation takes the form of a highly positive Si atom surrounded by negatively charged alkyl groups [62], which inhibits the solvation of a separated $R_3Si^+X^-$ ion pair [62]. Thus, while the ionic structure becomes lower than the covalent one, solvation is not expected to drastically lift the near-degeneracy of the covalent and ionic structures in the vicinity of the equilibrium distance. Consequently, the large resonance energy due to covalent–ionic mixing will create a deep minimum for the bond with a high barrier for heterolytic bond-breaking, as shown in Fig. 3b. Thus, the strong covalent–ionic resonance energy will glue the two fragments. In such a 1:1 species, even though the charge distribution in the Si–X bond may still appear ionic, this ionicity will remain virtual. Thus, SiR_3–X prefers to form discrete molecular structures, each of which is stabilized by covalent–ionic resonance over ion pairs stabilized by electrostatic attraction.

7 Conclusion

Although the great majority of quantitative calculations are done in the framework of MO theory, the language of chemists has remained faithful to VB theory. As such, the most commonly employed computational tool is not fully commensurate with a significant number of fundamental chemical concepts. This has occasionally created some confusion with respect to important paradigms of chemistry, such as resonance energy, Lewis structures, hybrid orbitals, mesomeric stuctures and so on. To take only a few examples, the role of electronic delocalization in aromaticity, the role of resonance in the rotational barriers of the peptide bonds in a protein or in the strength of carboxylic acids has long been debated, mainly because of the inadequacy of MO methods to relate faithfully to these VB-derived concepts.

Clearly, there has been a need for a computational method that would speak the language of chemists while being reasonably quantitative as far as geometries, force constants and energetics, in general, are concerned. The BOVB method is an endeavor to fill this gap by bringing

together the qualities of lucidity, compactness and reasonable accuracy. To achieve this accuracy, it is essential to take care of the differential electron-correlation types associated with the bonds that are created or broken along the reaction coordinate. A unique feature of the BOVB method is that it considers not only the Coulomb but also the dynamic part of this differential correlation, which can be very significant in some cases. The computational tests that have been performed in a variety of difficult cases show that the description is consistent and reasonably accurate, despite the extreme compactness of the wave functions.

The pictorial nature of BOVB allows the hierarchy of electron correlation effect to be charted and to be associated with the fundamental properties of the electron. Thus, the electron is a particle with a classical charge (e^-), a quantal particle with a spin, and is also a wave. Each of these properties leads to a characteristic correlation. Hartree–Fock theory takes care of the spin correlation by enabling electrons with identical spins to avoid one another (''Fermi holes''). However, Hartree–Fock theory neglects completely all other correlation effects. Correlated wave functions such as CASSCF, VBSCF, etc., take care of the Coulomb correlation due to the classical charge of the electron. Higher levels, for example, CASPT2, CCSD(T), VBCI, BOVB, etc., are required to account for the dynamic correlation, which is associated with the wave quality of the electrons and the ability of the probability density to respond instantaneously to local fields. VB theory (e.g., VBSCF, BOVB) shows very lucidly the nature of Coulomb correlation by preferring VB structures that keep away the electrons. BOVB shows most vividly that the dynamic correlation is the adaptation of the orbitals to the individual charges of the VB structures rather than to their mean field. We therefore contend that BOVB has a fundamental conceptual value, in addition to its accuracy.

The BOVB method is not designed, of course, to compete with the standard ab initio methods, but has its specific domain. The method serves as an interface between the quantitative rigor of today's capabilities and the traditional qualitative matrix of concepts of chemistry. As such, it has been mainly devised as a tool for computing diabatic states, with applications to chemical dynamics, chemical reactivity with the VB correlation diagrams, photochemistry, resonance concepts in organic chemistry, reaction mechanisms, and more generally all cases where a VB reading of the wave function or the properties of one particular VB structure are desirable in order to understand better the nature of an electronic state.

Acknowledgements. We thank all the collaborators and colleagues who contributed to the development of the BOVB method. These include P. Archirel, C. P. Byrman, D. Danovitch, J. M. Galbraith, N. Harris, S. Humbel, J. H. Langenberg, D. Lauvergnat, P. Maître, J. P. Malrieu, E. Noizet, W. Saunders, A. Shurki, J. H. van Lenthe and W. Wu.

References

1. (a) Pauling L (1931) J Am Chem Soc 53: 1367; (b) Pauling L (1932) J Am Chem Soc 54: 998; (c) Pauling L (1932) J Am Chem Soc 54: 3570; (d) Pauling L (1960) The nature of the chemical bond, 3rd edn. Cornell University Press, Ithaca, NY
2. (a) Slater JC (1930) Phys Rev 35: 509; (b) Slater JC (1931) Phys Rev 38: 1109; (c) Slater JC (1932) Phys Rev 41: 255
3. Wheland GW (1955) Resonance in organic chemistry. Wiley, New York
4. Hiberty PC (1998) J Mol Struct (THEOCHEM) 451: 237
5. Shaik SS (1981) J Am Chem Soc 103: 3692; (b) Pross A, Shaik SS (1983) Acc Chem Res 16: 363; (c) Pross A (1985) Adv Phys Org Chem 21: 99; (d) Pross A (1985) Acc Chem Res 18: 212; (e) Shaik SS (1989) In: Bertran J, Csizmadia IG (eds) New concepts for understanding organic reactions. NATO ASI series vol C267. Kluwer, Dordrecht; (f) Shaik SS, Hiberty PC (1991) In: ZB (ed) Theoretical models of chemical bonding, part 4. Springer, Berlin Heidelberg New York, pp 269–322; (g) Shaik SS (1985) Prog Phys Org Chem 15: 197; (h) Shaik S, Hiberty PC (1995) Adv Quantum Chem 26: 100
6. Shaik S, Shurki A (1999) Angew Chem Int Ed Engl 38: 586
7. (a) Sevin A, Hiberty PC, Lefour JM (1987) J Am Chem Soc 109: 1845; (b) Sevin A, Chaquin P, Hamon L, Hiberty PC (1988) J Am Chem Soc 110: 5681; (c) Sevin A, Giessner-Prettre C, Hiberty PC, Noizet E (1991) J Phys Chem 95: 8580.
8. (a) Bernardi F, Olivucci M, Robb MA (1992) J Am Chem Soc 114: 1606–1616; (b) Bernardi F, Olivucci M, Robb MA (1995) Pure Appl Chem 67: 17–24; (c) Garavelli M, Celani P, Bernardi F, Robb M. A, Olivucci M (1997) J Am Chem Soc.119: 6891–6901; (d) Michl J, Bonacic-Koutecky V (1990) Electronic aspects of organic photochemistry. Wiley, New York
9. (a) Shaik SS, Hiberty PC, Lefour JM, Ohanessian G (1987) J Am Chem Soc 109: 363; (b) Shaik SS, Hiberty PC, Ohanessian G, Lefour JM (1988) J Phys Chem 92: 5086; (c) Shaik S, Shurki A, Danovich D, Hiberty PC (1996) J Am Chem Soc 118: 666; (d) Shaik S, Shurki A, Danovich D, Hiberty PC (2001) Chem Rev 101: 1501–1539
10. Lauvergnat D, Hiberty PC (1997) J Am Chem Soc 119: 9478
11. Hiberty PC, Byrman CP (1995) J Am Chem Soc 117: 9875
12. da Motta Neto JD, Nascimento MAC (1996) J Phys Chem 100: 15105
13. (a) Hwang JK, King G, Creighton S, Warshel A (1988) J Am Chem Soc 110: 5297; (b) Shaik SS (1984) J Am Chem Soc 106: 1227
14. Hiberty PC, Flament JP, Noizet E (1992) Chem Phys Lett 189: 259
15. Hiberty PC, Humbel S, Byrman CP, van Lenthe JH (1994) J Chem Phys 101: 5969
16. Hiberty PC, Humbel S, Archirel P (1994) J Phys Chem 98: 11697
17. (a) Hiberty PC (1997) J Mol Struct (THEOCHEM) 398: 35; (b) Hiberty PC (1997) In: Davidson ER (ed) Modern electronic structure theory and applications in organic chemistry. World Scientific, River Edge, NJ, pp 289–367; (c) Hiberty PC, Shaik S (2002) In: Cooper DL, Klein DJ (eds) Valence bond theory. Theoretical and computational chemistry, vol 10. Elsevier, Amsterdam, pp 187–225
18. Lauvergnat D, Maître P, Hiberty PC, Volatron F (1996) J Phys Chem 100: 6463
19. Galbraith JM, Blank E, Shaik S, Hiberty PC (2000) Chem Eur J 6: 2425
20. Langenberg JH, Rutink PJA (1993) Theor Chim Acta 85: 285
21. Humbel S, Demachy I, Hiberty PC (1995) Chem Phys Lett 247: 126
22. Basch H, Wolk JL, Hoz S (1997) J Phys Chem A 101: 4996
23. Basch H, Aped P, Hoz S (1996) Mol Phys 89: 331
24. Shaik S, Wu W, Dong K, Song L, Hiberty PC (2001) J Phys Chem A 105: 8226.
25. (a) Hiberty PC, Leforestier C (1978) J Am Chem Soc 100: 2012; (b) Hiberty PC, Ohanessian G (1985) Int J Quantum Chem 27: 259
26. Heitler H, London F (1927) Z Phys 44: 455
27. (a) van Lenthe JH, Balint-Kurti GG (1980) Chem Phys Lett 76: 138; (b) van Lenthe JH, Balint-Kurti GG (1983) J Chem Phys

78: 5699; (c) Benneyworth PR, Balint-Kurti GG, Davis MJ, Williams IH (1992) J Phys Chem 96: 4346
28. Coulson CA, Fischer I (1949) Philos Mag 40: 386
29. (a) Hunt WJ, Hay PJ, Goddard WA III (1972) J Chem Phys 57: 738; (b) Goddard WA III, Harding LB (1978) Annu Rev Phys Chem 29: 363; (c) Bobrowicz FB, Goddard WA III (1977) In: Schaefer HF (ed) Methods of electronic structure theory. Plenum, New York, pp 79–127
30. Ladner RC, Goddard WA III (1969) J Chem Phys 51: 1073
31. Cooper DL, Gerratt J, Raimondi M (1987) Adv Chem Phys 69: 319; (b) Cooper DL, Gerratt J, Raimondi M (1988) Int Rev Phys Chem 7: 59; (c) Cooper DL, Gerratt J, Raimondi M (1990) In: Klein DJ, Trinajstic N (eds) Valence bond theory and chemical structure. Elsevier, Amsterdam, p 287; (d) Cooper DL, Gerratt J, Raimondi M (1990) Top Curr Chem 153: 41; (e) Karadakov PB, Gerratt J, Cooper DL, Raimondi M (1991) Chem Rev 91: 929
32. (a) Verbeek J (1990) PhD thesis. University of Utrecht; (b) Verbeek J, van Lenthe JH (1991) J Mol Struct (THEOCHEM) 229: 115; (c) Verbeek J, van Lenthe JH (1991) Int J Quantum Chem 40: 201
33. Verbeek J, Langenberg JH, Byrman CP, van Lenthe JH (1983) TURTLE – an ab initio VB/VBSCF/VBCI program. Theoretical Chemistry Group, Debye Institute, University of Utrecht
34. Lepetit MB, Malrieu JP (1993) J Phys Chem 97: 94
35. Jackels CF, Davidson ER (1976) J Chem Phys 64: 2908
36. (a) Voter AF, Goddard WA III (1981) Chem Phys 57: 253; (b) Voter AF, Goddard WA III (1981) J Chem Phys 75: 3638; (c) Voter AF, Goddard WA III (1986) J Am Chem Soc 108: 2830
37. (a) Hollauer E, Nascimento MAC (1991) Chem Phys Lett 184: 470; (b) Hollauer E, Nascimento MAC (1993) J Chem Phys 99: 1207; (c) Hollauer E, Nascimento MAC (1993) Chem Phys 177: 79; (d) Bielscowsky CE, Nascimento MAC, Hollauer E (1992) Phys Rev A 43: 7942
38. Murphy RB, Messmer RP (1993) J Phys Chem 98: 7958
39. Ohanessian G, Hiberty PC (1987) Chem Phys Lett 137: 437
40. Laidig WD, Saxe P, Bartlett RJ (1987) J Chem Phys 86: 887
41. Merchan M, Daudey JP, Gonzales-Luque R, Nebot-Gil (1990) J Chem Phys 141: 285
42. Huber KP, Herzberg G (1979) Molecular spectra and molecular structures. IV. Constants of diatomic molecules. van Nostrand Reinhold, New York
43. Hiberty PC, Lefour JM (1987) J Chim Phys 84: 607
44. Bauschlicher CW, Taylor PR (1987) J Chem Phys 86: 887
45. Bauschlicher CW, Langhoff SR, Taylor PR, Handy NC, Knowles PJ (1986) J Chem Phys 85: 1469
46. Schilling JB, Goddard WA III, Beauchamp JL (1987) J Phys Chem 91: 5616
47. Ohanessian G, Goddard WA III (1990) Acc Chem Res 23: 386
48. Galbraith GM, Shurki A, S. Shaik S (2000) J Phys Chem A 104: 1262
49. Petterson LGM, Bauschlicher CW, Langhoff SR, Partridge H (1987) J Chem Phys 87: 481
50. Clark T (1988) J Am Chem Soc 110: 1672
51. Gill PMW, Radom L (1988) J Am Chem Soc 110: 4931
52. (a) Pauling L (1931) J Am Chem Soc 53: 3225; (b) Pauling L (1933) J Chem Phys 1: 56
53. Nguyen MT, Ha T-K (1987) J Phys Chem 91: 1703
54. Braïda B, Hiberty PC (2000) J Phys Chem A 104: 4618
55. Braïda B, Lauvergnat D, Hiberty PC (2001) J Chem Phys 115: 90
56. McLean AD, Lengsfield III BH, Pacansky J, Ellinger Y (1985) J Chem Phys 83: 3567
57. Xie Y, Allen WD, Yamaguchi Y, Schaefer HF III (1996) J Chem Phys 104: 7615
58. Albu TV, Corchodo JC, Truhlar DG (2001) J Phys Chem A 105: 8465
59. O'Malley TF (1971) Adv At Mol Phys 7: 223
60. (a) Sini G, Maitre P, Hiberty PC, Shaik SS (1991) J Mol Struct (THEOCHEM) 229: 163; (b) Shaik SS (1991) In: Maksic ZB, Eckert-Maksic M (eds) Molecules in natural science and medicine. Ellis-Horwood, New York, pp 256–266
61. Shaik S, Maitre P, Sini G, Hiberty PC (1992) J Am Chem Soc 114: 7861
62. Shurki A, Hiberty PC, Shaik S (1999) J Am Chem Soc 121: 822
63. (a) Apeloig Y (1989) In: Patai S, Rappoport Z (eds) The chemistry of organic silicon compounds. Wiley, Chichester, p 57; (b) Apeloig Y (1987) Stud Org Chem 31: 33; (c) Apeloig Y, Merin-Aharoni O (1992) Croat Chem Acta 65: 757; (d) Lambert JB, Kania L, Zhang S (1995) Chem Rev 95: 1191; (e) Schwarz H (1989) In: Patai S, Rappoport Z (eds) The chemistry of organic silicon compounds, vol 1. Wiley, Chichester, pp 445–510
64. Corriu RJP, Henner M (1974) J Organomet Chem 74: 1
65. Eaborn C (1985) In: Sakurai H (ed) Organosilicon and bioorganosilicon chemistry. Ellis Horwood, UK
66. Olah GA, Heiliger L, Li X-Y, Prakash GKS (1990) J Am Chem Soc 112: 5991
67. Lickiss PD (1992) J Chem Soc Dalton Trans 1333
68. Prakash GKS, Keyaniyan S, Aniszfeld R, Heiliger L, Olah GA, Stevens RC, Choi H-K, Bau R (1987) J Am Chem Soc 109: 5123
69. Gomes de Mesquita AH, MacGillavry CH, Eriks K (1965) Acta Crystallogr 18: 437
70. Olah GA (1979) Top Curr Chem 80: 19
71. Xie Z, Liston DJ, Jelinek T, Mitro V, Bau R, Reed CA (1993) J Chem Soc Chem Commun 384
72. Lauvergnat D, Hiberty PC, Danovich D, Shaik S (1996) J Phys Chem 100: 5715
73. Pople JA, Head-Gordon M, Fox DJ, Raghavachari K, Curtiss LA (1989) J Chem Phys 90: 5622
74. Curtiss LA, Raghavachari K, Trucks G, Pople JA (1991) J Chem Phys 94: 7221
75. Armentrout PB, Beauchamp JL (1999) Acc Chem Res 22: 315
76. Langhoff SR, Bauschlicher Jr CW (1991) Chem Phys Lett 180: 13
77. Curtiss LA, Raghavachari K, Redfern PC, Pople JA (1997) J Chem Phys 106: 1063
78. NIST standard reference database no. 69, July 2001 release